Inorganic Chemistry
Article

Inorg. Chem. **2009**, *48*, 5129–5140 **5129**
DOI: 10.1021/ic8024556

Conjugate Base of a Secondary Phosphine Selenide $[P(Se)(O^iPr)_2]^-$ as the Bridging Unit for the Construction of Heterometallic Fe(II)−Hg(II)/Cd(II) Complexes

Bijay Sarkar,[†] Sung-Yin Wen,[†] Jyun-Hua Wang,[†] Ling-Song Chiou,[†] Ping-Kuei Liao,[†] Bidyut Kumar Santra,[†] Ju-Chun Wang,[‡] and C. W. Liu*[,†]

[†]*Department of Chemistry, National Dong Hwa University, Hualien, Taiwan 97401, Republic of China, and* [‡]*Department of Chemistry, Soochow University, Taipei, Taiwan 111, Republic of China*

Received December 29, 2008

Reactions of perchlorate salts of Hg(II)/Cd(II) with $[CpFe(CO)_2P(Se)(O^iPr)_2]$ (denoted as **L**) produced dicationic clusters $[HgL_2](ClO_4)_2$, **1**; $[HgL_3](ClO_4)_2$, **2**; and $[CdL_3(H_2O)](ClO_4)_2$, **11**. However, the reactions of **L** with Hg(II)/Cd(II) halides yielded neutral complexes. For instance, HgI_2 produced $[Hg_3I_6L_2]$, **3**, or $[HgI_2L_2]$, **4**, depending on the metal-to-ligand ratio used. Reaction of **L** with any of the Hg(II)/Cd(II) halides in a 1:1 ratio produced neutral clusters $[HgX(\mu\text{-}X)L]_2$ (M = Hg; X = Cl, **5**; Br, **6**; I, **7**; M = Cd; X = Cl, **8**; Br, **9**; I, **10**). Thus, variation of the M-to-**L** ratio made it possible for the formation of compounds with different metal/ligand stoichiometries only when ClO_4^- and I^- salts of Hg(II) were used. Single-crystal X-ray crystallography revealed that two and three **L** units were connected to a Hg(II) via its Se atom in **1** and **2**, respectively, whereas Hg(II) in **4** was connected to two "I" and two "**L**" units. An **L** (through its Se) and a terminal halogen were attached to each of the Hg(II)'s of the Hg_2X_2 parallelogram core in **5** and **6**. The cadmium complex **8**, with a Cd_2Cl_2 parallelogram core, was isostructural with the mercury complex **5**. Although bonding and connectivity in **8** were similar to those in **9** and **10**, the conformation of the bulky **L** ligands was unusually syn in **9** and **10**, unlike the anti orientation in **5**, **6**, and **8**. The syn conformation of **L** was also observed in compounds **1** and **2**. Secondary interactions, namely, Se···Se interaction, the X···H−C type of H-bonding (X = halogen or Se), and π-stacking, revealed in the structures played a role in determining the ligand conformation. The $[P(Se)(O^iPr)_2]^-$, the conjugate base of secondary phosphine selenide $[HP(Se)(O^iPr)_2]$, acted as a bridge with P bonded to Fe and Se bonded to Hg (or Cd) in these heterometallic clusters. Compound **5** further demonstrated a longer P−Se bond in the secondary phosphine selenide compared to that in isostructural, tertiary phosphine selenide metal complexes.

Introduction

Most of the metal complexes involving organoselenophosphorus ligands recorded in the Cambridge Structure Database are either tertiary phosphine selenide ($R_3P{=}Se$, where R includes substituted alkyl, aryl, alkoxyl, and phosphoramide)[1] or diselenophosphorus, namely, $[R_2PSe_2^-]$,[2] moieties which contain a phosphorus atom with a formal oxidation number of +5. Structural identification of metal complexes containing a conjugate base of secondary phosphine selenide $[R_2PSe]^-$, in which the formal oxidation number of P is +3, is scarce in the literature[3] due to the poor thermal stability of secondary phosphine selenide with respect to disproportionation. It should be noted that, even though tertiary phosphine selenide or diselenophosphorus units apparently contain a ($R_2P{=}Se$) moiety, their coordination chemistry can never be considered as similar to that of the secondary phosphine selenide.

On the other hand, the report of **L**,[4] the only structure containing a secondary selenophosphito $[(^iPrO)_2PSe]^-$ moiety, was possible because of its better stability achieved by P coordination on the iron carbonyl fragment, which is

*To whom correspondence should be addressed. Fax: +886-3-8633570. E-mail: chenwei@mail.ndhu.edu.tw.

(1) Representative examples: (a) Haiduc, I. *Comprehensive Coord. Chem. II*, 1st ed.; Lever, A. B. P., Ed.; Elsevier Ltd.: Oxford, U.K., 2004; Vol *1*, pp 323−347.(b) Lobana, T. S.; Rimple, A.; Turner, P. *Inorg. Chem.* **2003**, *42*, 4731–4737. (c) Gaunt, A. J.; Scott, B. L.; Neu, M. P. *Chem. Commun.* **2005**, 3215–3216. (d) German-Acacio, J. M.; Reyes-Lezama, M.; Zuniga-Villarreal, N. *J. Organomet. Chem.* **2006**, *691*, 3223–3231.

(2) Representative examples: (a) Lobana, T. S.; Wang, J.-C.; Liu, C. W. *Coord. Chem. Rev.* **2007**, *251*, 91–110. (b) Davies, R. P.; Francis, C. V.; Jurd, A. P. S.; Martinelli, M. G.; White, A. J. P.; Williams, D. J. *Inorg. Chem.* **2004**, *43*, 4802–4804. (c) Pilkington, M. J.; Slawin, A. M. Z.; Williams, D. J.; Woollins, J. D. *Polyhedron* **1991**, *10*, 2641–2645. (d) Nguyen, C. G.; Adeogun, A.; Afzaal, M.; Malik, M. A.; O'Brien, P. *Chem. Commun.* **2006**, 2182–2184.

(3) (a) Davies, R. P.; Martinelli, M. G. *Inorg. Chem.* **2002**, *41*, 348–352. (b) Han, H.; Johnson, S. A. *Organometallics* **2006**, *25*, 5594–5602. (c) Lindner, E.; Bosch, E.; Fawzi, R.; Steimann, M.; Mayer, H. A.; Gierling, K. *Chem. Ber.* **1996**, *129*, 945–951. (d) Zhang, Q.-F.; Cheung, F. K. M.; Wong, W.-Y.; Williams, I. D.; Leung, W.-H. *Organometallics* **2001**, *20*, 3777–3781. (e) Davies, R. P.; Martinelli, M. G.; White, A. J. P. *Chem. Commun.* **2006**, 3240–3042.

(4) Liu, C. W.; Chen, J.-M.; Santra, B. K.; Wen, S.-Y.; Liaw, B.-J.; Wang, J.-C. *Inorg. Chem.* **2006**, *45*, 8820–8822.

Published on Web 05/01/2009

reminiscent of the better stability of the P-coordinated secondary phosphine selenide.[5] The free Se end of **L** is capable of binding other metals to form heterometallic complexes, which afforded Fe(II)−Hg(II)/Cd(II)[4] as well as Fe(II)−Cu(I)/Ag(I)[6] heterometallic compounds, the only reported heterometallic structures containing a secondary phosphine selenide/selenophosphito unit to date. It is worth noting that only one compound, $[\{CpNi\{(OMe)_2PS\}_2\}_2Ni]$,[7] is known to involve its lighter congener, that is, the secondary thiophosphito $[(OR)_2PS]^-$ moiety.

Herein, we report the syntheses and structures of the heterometallic iron−mercury/ cadmium complexes (**1**−**11**) of a secondary selenophosphito ligand **L**, demonstrating the main structural difference with that of its tertiary counterpart in terms of bond distance, which differentiates the title compounds (**1**−**11**) from the numerous reported Hg(II)[8] and Cd(II)[9] compounds coordinated by the Se of $R_3P{=}Se$ and $R_2PSe_2^-$ units. Also highlighted is the formation of metallo supramolecules revealed in the lattices of some of the clusters via several types of secondary interactions, which are important classes of noncovalent forces and contribute to the self-assembly of building blocks to form supramolecular structures.[10]

Experimental Section

Materials and Measurements. All chemicals were purchased from commercial sources and used as received. Solvents were purified following standard protocols.[11] All of the reactions were performed in oven-dried Schlenk glassware by using standard inert-atmosphere techniques. $NH_4Se_2P(O^iPr)_2$[12] and **L**[4] were prepared according to the reported methods. The syntheses of $[Hg_3I_6L_2]$, **3**, and $[CdL_3(H_2O)](ClO_4)_2$, **11**, were reported earlier.[4] Commercial $Hg(ClO_4)_2\cdot xH_2O$, HgX_2 (X = Cl, Br, I) (99.9%), $Cd(ClO_4)_2\cdot 5H_2O$, and CdX_2 (X = Cl, Br, I) (99.9%) were purchased from Strem. The elemental analyses were done using a Perkin-Elmer 2400 CHN analyzer. NMR spectra were recorded on a Bruker Advance DPX300 FT-NMR spectrometer, which operates at 300 MHz while recording ^1H, 121.49 MHz while recording ^{31}P, and 57.24 MHz while recording ^{77}Se. The $^{31}P\{^1H\}$ and $^{77}Se\{^1H\}$ NMR are referenced externally against 85% H_3PO_4 (δ = 0 ppm) and PhSeSePh (δ = 463 ppm), respectively. The chemical shift (δ) and coupling constant (J) are reported in parts per million and hertz, respectively. The NMR spectra were recorded at ambient temperature if not mentioned. IR spectra were recorded on a JASCO FT-IR 401 spectrometer at 25 °C using KBr plates. Melting points were measured by using a Fargo MP-2D melting point apparatus. The cyclic voltammograms were recorded on a CH Instruments 611C electrochemical analyzer using a 0.5 mm Pt disk working electrode, Pt wire auxiliary electrode, and Ag/AgCl reference electrode and standardized by the redox couple ferricinium/ferrocene. ($^nBu_4N$)(PF_6) (0.1 M) was used as the supporting electrolyte, and acetonitrile was used as the solvent for all of the samples. All of the cyclic voltammetry measurements were carried out at 0.05 v/s scan rate.

Caution! *Selenium and its derivatives are toxic. These materials should be handled with great caution.*

Synthesis. $[Hg\{CpFe(CO)_2P(Se)(O^iPr)_2\}_2](ClO_4)_2$, 1. $Hg(ClO_4)_2\cdot xH_2O$ (0.06 g, 0.14 mmol) was added to a 50 mL acetone solution of $[CpFe(CO)_2P(Se)(O^iPr)_2]$ (0.11 g, 0.28 mmol) maintaining a 1:2 metal-to-ligand ratio in a flask at −20 °C and was stirred for 2 h. The solution was then evaporated to dryness to get a yellow oil. Ether was added to it to obtain **1** as a yellow solid, which was isolated by filtration. Yield: 0.12 g (68%). Mp: 129 °C (decomp.) Anal. calcd for $C_{26}H_{38}Cl_2Fe_2HgO_{16}P_2Se_2\cdot 2(CH_3)_2CO$: C, 28.99; H, 3.80. Found: C, 28.75; H, 3.55. ^1H NMR (DMSO-d_6): 1.50 (d, $^3J_{HH}$ = 4.52, 24H, CH_3), 4.93 (m, 4H, CH), 5.49 (m, 10H, Cp). ^{31}P NMR (DMSO-d_6, −60 °C): 182.3 ppm (s, $^2J_{PHg}$ = 50.6, $^1J_{PSe}$ = 492.1). ^{77}Se NMR (DMSO-d_6): 267.5 ppm (d, $^1J_{SeP}$ = 504.4). IR (cm^{-1}): 2044 and 1998 (υ_{CO}), 1099 (υ_{ClO4}), 525 (υ_{PSe}).

$[Hg\{CpFe(CO)_2P(Se)(O^iPr)_2\}_3](ClO_4)_2$, 2. A similar procedure to that described for **1** was adopted, though a 1:3 metal-to-ligand ratio was maintained; thus, 0.17 g (0.42 mmol) of **L** was used. Yield: 0.15 g (66%). Mp: 136 °C (decomp.) Anal. calcd for $C_{39}H_{57}Cl_2Fe_3HgO_{20}P_3Se_3$: C, 29.01; H, 3.56. Found: C, 29.26; H, 3.67. ^1H NMR (DMSO-d_6): 1.45 (d, $^3J_{HH}$ = 6.07, 36H, CH_3), 4.96 (m, 6H, CH), 5.58 (s, 15H, Cp). ^{31}P NMR (DMSO-d_6, −60 °C): 177.6 (s, $^2J_{PHg}$ = 132.4, $^1J_{PSe}$ = 573.8). ^{77}Se NMR (DMSO-d_6): 235.7 (d, $^1J_{SeP}$ = 574.7). IR (cm^{-1}): 2040 and 1994 (υ_{CO}), 1099 (υ_{ClO4}), 525 (υ_{PSe}).

$[HgI_2\{CpFe(CO)_2P(Se)(O^iPr)_2\}_2]$, 4. HgI_2 (0.11 g, 0.24 mmol) was added to a 50 mL acetone solution of **L** (0.19 g, 0.48 mmol) in a 100 mL flask and was stirred for 4 h at 0 °C. Then, it was filtered, and the filtrate was evaporated to dryness under vacuum conditions to get yellow oil, which solidified upon the addition of hexane. The solid was separated by filtration and washed with ether to obtain the product as a yellow solid. Yield: 0.14 g (47%). Mp: 128 °C. Anal. calcd for $C_{26}H_{38}Fe_2HgI_2O_8P_2Se_2$: C, 24.70; H, 3.03. Found: C, 24.94; H, 3.16. ^1H NMR (acetone-d_6): 1.41 (d, $^3J_{HH}$ = 6.12, 24H, CH_3), 5.00 (m, 4H, CH), 5.53 (br s, 10H, Cp). ^{31}P NMR (acetone-d_6): 171.9 (s, $^1J_{PSe}$ = 646.1). ^{77}Se NMR (acetone-d_6): 239.4 (d, $^1J_{SeP}$ = 643.9). IR (cm^{-1}): 2044, 1998 (υ_{CO}), 528 (υ_{PSe}).

$[HgCl(\mu\text{-}Cl)\{CpFe(CO)_2P(Se)(O^iPr)_2\}]_2$, 5. Synthesis was carried out by the same procedure described for **4**. However, $HgCl_2$ (0.13 g, 0.49 mmol) was used instead of HgI_2, and a 1:1 metal-to-ligand ratio was maintained. Yield: 0.17 g (52%). Mp: 69 °C. Anal. calcd for $C_{26}H_{38}Cl_4Fe_2Hg_2O_8P_2Se_2$: C, 23.08; H, 2.83. Found: C, 23.45; H, 2.97. ^1H NMR (DMSO-d_6): 1.15 (d, $^3J_{HH}$ = 5.73, 24H, CH_3), 4.87 (m, 4H, CH), 5.43 (s, 10H, Cp). ^{31}P NMR (DMSO-d_6): 176.9 (s, $^1J_{PSe}$ = 533.5). ^{77}Se NMR (DMSO-d_6): 219.2 (d, $^1J_{SeP}$ = 532.7). IR (cm^{-1}): 2050, 2006 (υ_{CO}), 517 (υ_{PSe}).

$[HgBr(\mu\text{-}Br)\{CpFe(CO)_2P(Se)(O^iPr)_2\}]_2$, 6. Compound **6** was prepared using a similar procedure to that described for **5**. But, $HgBr_2$ was used instead of $HgCl_2$. Yield: 0.23 g (61%). Mp: 112 °C. Anal. calcd for $C_{26}H_{38}Br_4Fe_2Hg_2O_8P_2Se_2$: C, 20.40; H,

(5) (a) Walther, B. *Coord. Chem. Rev.* **1984**, *60*, 67–105. (b) Davies, R. Chalcogen-Phosphorus (and Heavier Cogeners) Chemistry. In *Handbook of Chalcogen Chemistry- New Perspectives in Sulfur, Selenium and Tellurium*; Devillanova, F. A., Ed.; RSC: Cambridge, U.K.

(6) Santra, B. K.; Chen, J.-L.; Sarkar, B.; Liu, C. W. *Dalton Trans.* **2008**, 2270–2276.

(7) Klaui, W.; Schmidt, K.; Bockmann, A.; Brauer, D. J.; Wilke, J.; Lueken, H.; Elsenhans, U. *Inorg. Chem.* **1986**, *25*, 4125–4130.

(8) (a) Lobana, T. S. *Prog. Inorg. Chem.* **1989**, *37*, 495–588. (b) Lobana, T. S.; Hundal, R.; Singh, A.; Sehdev, A.; Turner, P.; Castineiras, A. *J. Coord. Chem.* **2002**, *55*, 353–362. (c) Crouch, D. J.; Hatton, P. M.; Helliwell, M.; O'Brien, P.; Raftery, J. *Dalton Trans.* **2003**, 2761–2766. (d) Lobana, T. S.; Singh, A.; Kaur, M.; Castineiras, A. *Proc. Indian Acad. Sci., Chem. Sci.* **2001**, *113*, 89–94. (e) Garcia-Montalvo, V.; Novosad, J.; Kilian, P.; Woollins, J. D.; Slawin, A. M. Z.; Garcia y Garcia, P.; Lopez-Cardoso, M.; Espinosa-Perez, G.; Cea-Olivares, R. *J. Chem. Soc., Dalton Trans.* **1997**, 1025–1030.

(9) (a) Liu, C.-W.; Lobana, T. S.; Santra, B. K.; Hung, C.-M.; Liu, H.-Y.; Liaw, B.-J.; Wang, J.-C. *Dalton Trans.* **2006**, 560–570. (b) Cupertino, D.; Birdsall, D. J.; Slawin, A. M. Z.; Woollins, J. D. *Inorg. Chim. Acta* **1999**, *290*, 1–7. (c) Afzaal, M.; Crouch, D.; Malik, M. A.; Motevalli, M.; O'Brien, P.; Park, J.-H. *J. Mater. Chem.* **2003**, *13*, 639–640. (d) Kramolowsky, R.; Sawluk, J.; Siasios, G.; Tiekink, E. R. T. *Inorg. Chim. Acta* **1998**, *269*, 317–321. (e) Gray, I. P.; Slawin, A. M. Z.; Woollins, J. D. *Dalton Trans.* **2005**, 2188–2194.

(10) Amabilino, D. V.; Stoddart, J. F. *Chem. Rev.* **1995**, *95*, 2725–2828.

(11) Perrin, D. D.; Armarego, W. L. F.; Perrin, D. R. *Purification of Laboratory Chemicals*, 2nd ed.; Pergamon Press: Oxford, U.K., 1980.

(12) Liu, C. W.; Shang, I.-J.; Hung, C.-M.; Wang, J.-C.; Keng, T.-C. *J. Chem. Soc., Dalton Trans.* **2002**, 1974–1979.

2.50. Found: C, 20.78; H, 2.79. ^{1}H NMR (DMSO-d_6): 1.29 (d, $^3J_{HH}$ = 6.06, 24H, CH_3), 4.81 (m, 4H, C*H*), 5.44 (s, 10H, Cp). ^{31}P NMR (DMSO-d_6): 176.5 (s, $^1J_{PSe}$ = 548.7). ^{77}Se NMR (DMSO-d_6): 234.8 (d, $^1J_{SeP}$ = 546.1). IR (cm^{-1}): 2050, 2004 (υ_{CO}), 525 (υ_{PSe}).

[HgI(μ-I){CpFe(CO)$_2$P(Se)(O^{i}Pr)$_2$}]$_2$, 7. The dark yellow gummy product was obtained using a similar procedure to that described for **5** but using HgI_2 instead of $HgCl_2$. Yield: 0.37 g (87%). Anal. calcd for $C_{26}H_{38}Fe_2Hg_2I_4O_8P_2Se_2 \cdot 0.5(CH_3)_2CO$: C, 18.90; H, 2.36. Found: C, 18.90; H, 2.44. ^{1}H NMR (acetone-d_6): 1.41 (d, $^3J_{HH}$ = 6.11, 24H, CH_3), 5.00 (m, 4H, C*H*), 5.55 (s, 10H, Cp). ^{31}P NMR (acetone-d_6): 175.7 (s, $^1J_{PSe}$ = 570.9). ^{77}Se NMR (acetone-d_6): 268.0 (d, $^1J_{SeP}$ = 570.6). IR (cm^{-1}): 2048, 2006 (υ_{CO}), 528 (υ_{PSe}).

[CdCl(μ-Cl){CpFe(CO)$_2$P(Se)(O^{i}Pr)$_2$}]$_2$, 8. $CdCl_2$ (0.11 g, 0.60 mmol) was added to a 30 mL acetone solution of **L** (0.24 g, 0.60 mmol). The mixture was stirred in an ice bath for 1 h. The solution was filtered, and the filtrate was evaporated to dryness under vacuum conditions to get the product as a yellowish-brown solid. Single crystals were grown from the CH_2Cl_2 solution of the compound. Yield: 0.29 g (82%). Mp: 170 °C (decomp.). Anal. calcd for $C_{26}H_{38}Cd_2Cl_4Fe_2O_8P_2Se_2 \cdot 1.5\,CH_2Cl_2$: C, 25.33; H, 3.17. Found: C, 25.48; H, 3.19. ^{1}H NMR (acetone-d_6): 1.23(d, $^3J_{HH}$ = 8.16, 12H, CH_3), 4.87 (m, 2H, C*H*), 5.03 (s, 5H, Cp). ^{31}P NMR (acetone-d_6): 169.3 ($^1J_{PSe}$ = 698.4). ^{77}Se NMR (acetone-d_6): 167.5 (d, $^1J_{PSe}$ = 657.7), 172.4 (d, $^1J_{PSe}$ = 667.3). IR (cm^{-1}): 1997, 2043 (υ_{CO}), 528 (υ_{PSe}).

[CdBr(μ-Br){CpFe(CO)$_2$P(Se)(O^{i}Pr)$_2$}]$_2$, 9. Compound **9** was obtained using a similar procedure to that described for **8**, but $CdBr_2$ was used instead of $CdCl_2$. Yield: 0.32 g (78%). Mp: 140 °C (decomp.). Anal. calcd for $C_{26}H_{38}Cd_2Br_4Fe_2O_8P_2Se_2$: C, 23.05; H, 2.83. Found: C, 22.75; H, 3.14. ^{1}H NMR (acetone-d_6): 1.40 (d, $^3J_{HH}$ = 5.67, 12H, CH_3), 4.95 (m, 2H, C*H*), 5.51 (s, 5H, Cp). ^{31}P NMR (acetone-d_6): 176.6 ($^1J_{PSe}$ = 588.8). ^{77}Se NMR (acetone-d_6): 145.0 (d, $^1J_{PSe}$ = 587.6). IR (cm^{-1}): 2005, 2049 (υ_{CO}), 530 (υ_{PSe}).

[CdI(μ-I){Cp(CO)$_2$FeP(Se)(O^{i}Pr)$_2$}]$_2$, 10. Compound **10** was obtained using a similar procedure to that described for **8**, but CdI_2 was used instead of $CdCl_2$. Yield: 0.36 g (76%). Mp: 146 °C (decomp.). Anal. calcd for $C_{26}H_{38}Cd_2I_4Fe_2O_8P_2Se_2$: C, 20.24; H, 2.48. Found: C, 20.11; H, 2.49. ^{1}H NMR (acetone-d_6): 1.41 (d, $^3J_{HH}$ = 5.73, 12H, CH_3), 5.00 (m, 2H, C*H*), 5.51 (s, 5H, Cp). ^{31}P NMR (acetone-d_6): 175.9 ($^1J_{PSe}$ = 598.4). ^{77}Se NMR (acetone-d_6): 165.5 (d, $^1J_{PSe}$ = 598.6). IR (cm^{-1}): 2005, 2049 (υ_{CO}), 530 (υ_{PSe}).

X-Ray Crystallographic Procedures. Single crystals suitable for X-ray diffraction were grown by diffusing hexane into the acetone solution of the compounds (except **8**; see the Synthesis section). Crystals were mounted on the tips of glass fibers with epoxy resin. Data were collected on a P4 diffractometer for **1** and **2** and the rest of compounds on an APEX II diffractometer, using graphite monochromated Mo Kα radiation (λ = 0.71073 Å). Data reduction was performed with XSCANS[13] and SAINT,[14] which corrects for Lorentz and polarization effects. Empirical absorption corrections based on Ψ scans for **1** and **2** and multiscan (SADABS was used) for the rest of the compounds were performed. Due to the very weak intensity of high-angle data of **1**, diffraction data were only collected to $2\Theta \sim 45$ °. A relatively large value for the second parameter in the weighting scheme might be due to the unsolved disordered problems on the alkyl side chains. Two chlorine atoms (Cl1 and Cl3) of the perchlorate anions in **2** were located in special positions. Hence, all oxygen atoms connected to both Cl1 and Cl3 atoms are found to be disordered. Each is treated in 50% occupancy, and the Cl−O distances are constrained at 1.40(1) Å. Relatively large solvent-accessible voids are observed in **2** and **4**. Since the final difference map for these two structures is quite flat, the voids could be due to unsolved disorder problems on the alkyl side chains. Cell parameters for **5** possess a relatively large deviation because of poor crystal quality. Some residual electron densities, which could be ghost peaks, are identified at a distance of ~1.059 Å from the mercury atom in **5**. Alkyl side chains of the compounds are found to be more or less disordered, which is commonly observed for the ligand used. An effort has been made to resolve the problem concerning disordered side chains as much as possible. However, only a few of them could be solved properly. All H atoms were added in idealized positions. Structures were solved by the use of direct methods, and refinement was performed by the least-squares methods on F^2 with the SHELXL-97 package,[15] incorporated in SHELXTL/PC V5.10.[16] Crystal data and selected bond lengths and angles for **1**, **2**, **4**−**6** are summarized in Tables 1 and 2, while those for **8**−**10** are summarized in Tables 3 and 4, respectively. Crystallographic data of **3** and **11** were reported previously.[4]

Results and Discussion

The complexation of [CpFe(CO)$_2$P(Se)(O^{i}Pr)$_2$] (**L**) with perchlorate and halide salts of Hg(II) in different molar ratios is presented in Scheme 1. While the reaction of **L** with Hg$(ClO_4)_2$ in a 2:1 ratio produces [HgL$_2$]$(ClO_4)_2$ (**1**) in 68% yield, the reaction at a 3:1 ratio results in [HgL$_3$]$(ClO_4)_2$, **2**, in 66% yield. However, the complexation of **L** with HgI_2 in a 2:1 ratio produces [HgI$_2$L$_2$], **4**, in a 47% yield, whereas that in a 3:2 ratio yields [Hg$_3$I$_4$(μ-I)$_2$L$_2$], **3**.[4] On the other hand, HgX_2 (X = Cl, Br, I) reacts with **L** in a 1:1 ratio to form [HgX(μ-X)L]$_2$ [X = Cl, **5**; Br, **6**; I, **7**]. Treatment of **L**, with CdX_2 in a 1:1 ratio, affords three compounds with a general formula of [CdX(μ-X)L]$_2$ [X = Cl, **8**; Br, **9**; I, **10**]. However, the reaction of **L** with perchlorate salts of cadmium produces [Cd(L)$_3$(H$_2$O)]$(ClO_4)_2$, **11** (Scheme 1).[4] All of the compounds are characterized by multinuclear (^{1}H, ^{31}P, ^{77}Se) NMR and IR spectroscopy and elemental analyses. Single-crystal X-ray diffraction studies enabled structural elucidations for compounds **1**−**6** and **8**−**10**.

Structures. Compound 1. Compound **1** crystallizes in a monoclinic space group $P2_1/c$. Two Se atoms from two **L**'s coordinate to the Hg atom in an almost linear fashion [Se1−Hg−Se2, 166.95(7)°]. The bivalent mercury is connected to two Fp fragments (Fp = CpFe(CO)$_2$) by the bridging [(O^{i}Pr)$_2$PSe]$^-$ unit to form a dicationic, heterometallic complex. The asymmetric unit also contains two perchlorates as counteranions. Hg−Se bond lengths [2.4577(17), 2.4598(18) Å] are slightly shorter than the 2.471(2) Å reported in [Hg(SePh)$_2$][17] and, indeed, are the shortest in this series (**1**−**7**). P−Se distances, 2.228(4) and 2.231(4) Å, are in their normal range. One of the isopropoxyl O atoms from each of the **L** ligands (O2 and O3) shows weak interactions with the Hg, evident from the Hg1···O2 and Hg1···O3 distances of 2.893(14) and 2.868(12) Å, respectively. The perchlorate oxygen atom, O18, also displays a strong

(13) *XSCANS*, release 2.21; Siemens Energy and Automation, Inc.: Madison, WI, 1995.

(14) *SAINT*, V4.043; Bruker Analytical X-ray System: Madison, WI, 1995.

(15) Sheldrick, G. M. *SHELXL-97*; University of Göttingen: Göttingen, Germany, 1997.

(16) *SHELXL 5.10 (PC version)*; Bruker Analytical X-ray System: Maidson, WI, 1998.

(17) Lang, E. S.; Dias, M. M.; Abram, U.; Vazquez-Lopez, E. M. *Z. Anorg. Allg. Chem.* **2000**, *626*, 784–788.

Table 1. Selected Crystallographic Data for Compounds **1**, **2**, **4**−**6**

	1	**2**	**4**	**5**	**6**
formula	$C_{26}H_{38}Cl_2$ Fe_2HgO_{16} P_2Se_2	$C_{39}H_{57}Cl_2$ $Fe_3HgO_{20}P_3Se_3$	$C_{52}H_{76}Fe_4Hg_2$ $I_4O_{16}P_4Se_4$	$C_{26}H_{38}Cl_4Fe_2$ $Hg_2O_8P_2Se_2$	$C_{13}H_{19}Br_2$ $FeHgO_4PSe$
fw	1209.61	1614.68	2529.03	1353.10	765.47
space group	$P2_1/c$	$P\bar{1}$	$P\bar{1}$	$P\bar{1}$	$P\bar{1}$
a, Å	10.800(2)	14.7854(14)	14.5017(8)	8.486(7)	8.4692(6)
b, Å	11.8528(18)	15.134(2)	16.9017(9)	9.616(8)	9.6595(7)
c, Å	31.653(6)	17.578(3)	18.8419(10)	14.280(17)	14.6288(11)
α, deg	90	71.037(13)	70.113(2)	100.46(3)	101.9110(10)
β, deg	91.226(15)	65.262(11)	89.403(2)	92.42(3)	91.1600(10)
γ, deg	90	60.928(10)	75.863(2)	112.928(19)	112.7130(10)
V, Å^3	4050.8(12)	3085.4(7)	4197.9(4)	1047.2(17)	1073.54(14)
Z	4	2	2	1	2
ρ_{calcd}, g cm^{-3}	1.983	1.738	2.001	2.146	2.368
μ, mm^{-1}	6.559	5.168	7.648	10.095	13.321
T, K	293(2)	293(2)	298(2)	293(2)	273(2)
reflns collected	6934	11651	25567	7615	10843
independent reflns	5252 (R_{int} = 0.0654)	10299 (R_{int} = 0.0399)	14669 (R_{int} = 0.0607)	3358 (R_{int} = 0.0466)	3661 (R_{int} = 0.0340)
final R indices [$I > 2\sigma(I)$][a,b]	$R1$ = 0.0612	$R1$ = 0.0680	$R1$ = 0.0605	$R1$ = 0.0554	$R1$ = 0.0292
	$wR2$ = 0.1335	$wR2$ = 0.1639	$wR2$ = 0.1036	$wR2$ = 0.1459	$wR2$ = 0.0732
R indices (all data)[a,b]	$R1$ = 0.0936	$R1$ = 0.1260	$R1$ = 0.1431	$R1$ = 0.0644	$R1$ = 0.0339
	$wR2$ = 0.1606	$wR2$ = 0.2002	$wR2$ = 0.1155	$wR2$ = 0.1522	$wR2$ = 0.0749
goodness of fit	1.083	1.112	1.027	1.016	1.067
largest diff. peak and hole, e/Å^3	1.434 and −2.868	1.285 and −1.843	1.337 and −0.835	2.795 and −2.492	0.856 and −1.022

[a] $R1 = \sum||F_o| - |F_c||/\sum|F_o|$. [b] $wR2 = \{\sum[w(F_o^2 - F_c^2)^2]/\sum[w(F_o^2)^2]\}^{1/2}$.

Table 2. Bond Lengths (Å) and Angles (deg) in **1**, **2**, **4**−**6** with esd's in Parentheses

			Complex **1**		
Hg(1)−Se(1)	2.4577(17)	Hg(1)−Se(2)	2.4598(18)	P(1)−Se(1)	2.228(4)
P(2)−Se(2)	2.231(4)				
Se(1)−Hg(1)−Se(2)	166.95(7)	P(1)−Se(1)−Hg(1)	95.35(12)	P(2)−Se(2)−Hg(1)	94.00(11)
			Complex **2**		
Hg(1)−Se(2)	2.5208(14)	Hg(1)−Se(1)	2.5322(16)	Hg(1)−Se(3)	2.5375(14)
Se(1)−P(1)	2.218(4)	Se(2)−P(2)	2.197(3)	Se(3)−P(3)	2.200(3)
Se(2)−Hg(1)−Se(1)	120.48(5)	Se(2)−Hg(1)−Se(3)	120.25(5)	Se(1)−Hg(1)−Se(3)	118.91(5)
P(1)−Se(1)−Hg(1)	106.66(11)	P(2)−Se(2)−Hg(1)	107.77(10)	P(3)−Se(3)−Hg(1)	106.67(9)
			Complex **4**		
Hg(1)−Se(1)	2.6449(13)	Hg(1)−I(2)	2.7094(11)	Hg(1)−Se(2)	2.7681(13)
Hg(1)−I(1)	2.7776(10)	Hg(2)−Se(4)	2.6394(14)	Hg(2)−I(3)	2.7044(10)
Hg(2)−Se(3)	2.7675(12)	Hg(2)−I(4)	2.7785(11)	Se(2)−P(2)	2.161(3)
Se(3)−P(3)	2.168(3)	Se(1)−P(1)	2.176(3)	Se(4)−P(4)	2.172(3)
Se(1)−Hg(1)−Se(2)	86.71(4)	I(2)−Hg(1)−I(1)	108.87(4)	Se(4)−Hg(2)−Se(3)	88.45(4)
I(3)−Hg(2)−I(4)	109.37(4)	P(2)−Se(2)−Hg(1)	119.40(9)	P(3)−Se(3)−Hg(2)	118.69(9)
P(1)−Se(1)−Hg(1)	104.90(9)	P(4)−Se(4)−Hg(2)	106.06(9)		
			Complex **5**		
Hg(1)−Cl(1)	2.392(4)	Hg(1)−Se(1)	2.4931(19)	Hg(1)−Cl(3)	2.610(3)
Hg(1)−Cl(3A)	2.742(4)	Se(1)−P(1)	2.229(3)		
Cl(1)−Hg(1)−Se(1)	135.86(9)	Cl(1)−Hg(1)−Cl(3)	105.47(13)	Se(1)−Hg(1)−Cl(3)	108.15(9)
Cl(1)−Hg(1)−Cl(3A)	101.73(11)	Se(1)−Hg(1)−Cl(3A)	108.22(9)	Cl(3)−Hg(1)−Cl(3A)	86.16(9)
P(1)−Se(1)−Hg(1)	97.55(8)	Hg(1)−Cl(3)−Hg(1A)	93.84(9)		
			Complex **6**		
Hg(1)−Br(2)	2.5043(7)	Hg(1)−Se(1)	2.5151(6)	Hg(1)−Br(1A)	2.7184(6)
Hg(1)−Br(1)	2.8745(6)	Se(1)−P(1)	2.2276(13)		
Br(2)−Hg(1)−Se(1)	130.93(2)	Br(2)−Hg(1)−Br(1A)	107.28(2)	Se(1)−Hg(1)−Br(1A)	110.71(2)
Br(2)−Hg(1)−Br(1)	102.55(2)	Se(1)−Hg(1)−Br(1)	108.99(2)	Br(1A)−Hg(1)−Br(1)	87.395(17)
Hg(1A)−Br(1)−Hg(1)	92.605(17)	P(1)−Se(1)−Hg(1)	99.84(4)		

van der Waals contact with the mercury center, evident from the O18···Hg nonbonding distance of 2.987(20) Å. In addition, the secondary Se···Se interaction between two Se1 atoms of the neighboring molecules formed a loosely bound, dimeric supramolecule (Figure 1). The Se1···Se1 distance of 3.736(2) Å is less than twice that of

Table 3. Selected Crystallographic Data for Compounds **8**−**10**

	8	**9**	**10**
formula	$C_{13}H_{19}CdCl_2FeO_4PSe$	$C_{26}H_{38}Br_4Cd_2Fe_2O_8P_2Se_2$	$C_{13}H_{19}CdFeI_2O_4PSe$
fw	588.36	1354.56	771.26
space group	$P2_1/c$	$P2_1/c$	$Pbcn$
a, Å	13.547(8)	14.8691(9)	8.1713(3)
b, Å	9.094(6)	15.1994(9)	20.2209(7)
c, Å	17.277(11)	19.7322(13)	27.2425(9)
β, deg	92.274(14)	102.003(2)	90
V, Å^3	2127(2)	4362.0(5)	4501.3(3)
Z	4	4	8
ρ_{calcd}, g cm^{-3}	1.838	2.063	2.276
μ, mm^{-1}	3.731	7.058	6.032
T, K	273(2)	273(2)	223(2)
reflns collected	17193	48653	33242
independent reflns	3771 (R_{int} = 0.0989)	10861 (R_{int} = 0.0683)	3863 (R_{int} = 0.0803)
final R indices [$I > 2\sigma(I)$][a,b]	$R1$ = 0.0463	$R1$ = 0.0513	$R1$ = 0.0360
	$wR2$ = 0.0849	$wR2$ = 0.1135	$wR2$ = 0.0756
R indices (all data)[a,b]	$R1$ = 0.1022	$R1$ = 0.0943	$R1$ = 0.0579
	$wR2$ = 0.0994	$wR2$ = 0.1318	$wR2$ = 0.0830
goodness of fit	0.945	1.014	1.060
largest diff. peak and hole, e/ Å^3	0.894 and −0.596	1.571 and −1.606	1.431 and −0.525

[a] $R1 = \sum||F_o| - |F_c||/\sum|F_o|$. [b] $wR2 = \{\sum[w(F_o^2 - F_c^2)^2]/\sum[w(F_o^2)^2]\}^{1/2}$.

Table 4. Selected Bond lengths (Å) and Angles (deg) in **8**−**10** with esd's in Parentheses

		Complex **8**			
Cd(1)−Cl(1)	2.410(2)	Cd(1)−Cl(2)	2.494(2)	Cd(1)−Se(1)	2.5771(16)
Cd(1)−Cl(2A)	2.623(2)	Se(1)−P(1)	2.187(2)		
Cl(1)−Cd(1)−Cl(2)	111.18(8)	Cl(1)−Cd(1)−Se(1)	118.27(6)	Cl(2)−Cd(1)−Se(1)	124.00(7)
Cl(1)−Cd(1)−Cl(2A)	102.70(9)	Cl(2)−Cd(1)−Cl(2A)	87.91(7)	Se(1)−Cd(1)−Cl(2A)	104.61(6)
P(1)−Se(1)−Cd(1)	97.31(6)	Cd(1)−Cl(2)−Cl(1A)	92.09(7)		
		Complex **9**			
Cd(1)−Br(1)	2.5110(9)	Cd(1)−Se(1)	2.5925(7)	Cd(1)−Br(2)	2.6745(8)
Cd(1)−Br(3)	2.7488(9)(9)	Cd(2)−Br(4)	2.5207(8)	Cd(2)−Se(2)	2.6033(8)
Cd(2)−Br(3)	2.6214(9)	Cd(2)−Br(2)	2.7274(8)	Se(1)−P(1)	2.1836(15)
Se(2)−P(2)	2.1738(16)				
Br(1)−Cd(1)−Se(1)	125.13(3)	Br(1)−Cd(1)−Br(2)	115.62(3)	Se(1)−Cd(1)−Br(2)	112.11(3)
Br(1)−Cd(1)−Br(3)	107.01(3)	Se(1)−Cd(1)−Br(3)	97.97(3)	Br(2)−Cd(1)−Br(3)	90.41(2)
Br(4)−Cd(2)−Se(2)	121.87(3)	Br(4)−Cd(2)−Br(3)	116.56(3)	Se(2)−Cd(2)−Br(3)	116.47(3)
Br(4)−Cd(2)−Br(2)	102.85(3)	Se(2)−Cd(2)−Br(2)	97.35(2)	Br(3)−Cd(2)−Br(2)	92.02(3)
P(1)−Se(1)−Cd(1)	93.82(4)	P(2)−Se(2)−Cd(2)	94.47(5)	Cd(1)−Br(2)−Cd(2)	86.29(2)
Cd(2)−Br(3)−Cd(1)	86.90(2)				
		Complex **10**			
Cd(1)−Se(1)	2.6066(8)	Cd(1)−I(2)	2.6960(7)	Cd(1)−I(1)	2.8452(6)
Cd(1)−I(1A)	2.9124(7)	Se(1)−P(1)	2.1857(16)		
Se(1)−Cd(1)−I(2)	119.86(3)	Se(1)−Cd(1)−I(1)	112.20(2)	I(2)−Cd(1)−I(1)	117.79(2)
Se(1)−Cd(1)−I(1A)	95.70(2)	I(2)−Cd(1)−I(1A)	112.98(2)	I(1)−Cd(1)−I(1A)	92.237(19)
Cd(1)−I(1)−Cd(1A)	83.894(19)	P(1)−Se(1)−Cd(1)	97.13(5)		

the van der Waals radii of selenium (4.0 Å)[18] and the reported values for this type of interaction.[19]

It is to be noted that a two-coordinate Hg(II) center connected to two Se atoms was found only in $Hg(SePh)_2$,[17] $[Hg_7Se_{10}]_n^{4-}$,[20] and $[Hg_7Se_9]_n^{4n-}$.[20]

Compound 2. A perspective view of the cation is shown in Figure 2a. It crystallizes in the triclinic $P\bar{1}$ space group. Three **L**'s utilize their Se atoms to coordinate to the central Hg atom in near trigonal-planar geometry, evident from the Se−Hg−Se bond angles of 120.48(5), 120.25(5), and 118.91(5)°, though the Hg atom is situated only 0.089(1) Å above the Se_3 plane. The Hg—Se lengths, 2.5208(14)−2.5375(14) Å, are in the same range as those observed in $[Hg\{SeC(O)Tol\}_3]^-$ (2.5433(5)−2.5867(5) Å).[21] All three P−Se−Hg angles 106.66(11)−107.77(10)° are larger than those observed in compound **3**.[4] P−Se distances, 2.197(3)−2.218(4) Å, shorter than those observed in **1** suggest a larger bond order in **2** and are in good agreement with $^{31}P-^{77}Se$ coupling constants obtained from solution NMR studies (vide infra).

Interestingly, $\pi-\pi$ interactions of two Cp rings revealed between the adjacent cationic units lead to the formation

(18) Lange, N. A. *Lange's Handbook of Chemistry*, 11th ed.; McGraw-Hill: New York, 1973.

(19) Shi, W.; Kelting, R.; Shafaei-Fallah, M.; Rothenberger, A. *J. Organomet. Chem.* **2007**, *692*, 2678–2682.

(20) Kim, K.-W.; Kanatzidis, M. G. *Inorg. Chem.* **1991**, *30*, 1966–1969.

(21) Tack, M. N.; Dean, P. A. W.; Vittal, J. J. *Dalton Trans.* **2004**, 2890–2894.

Scheme 1

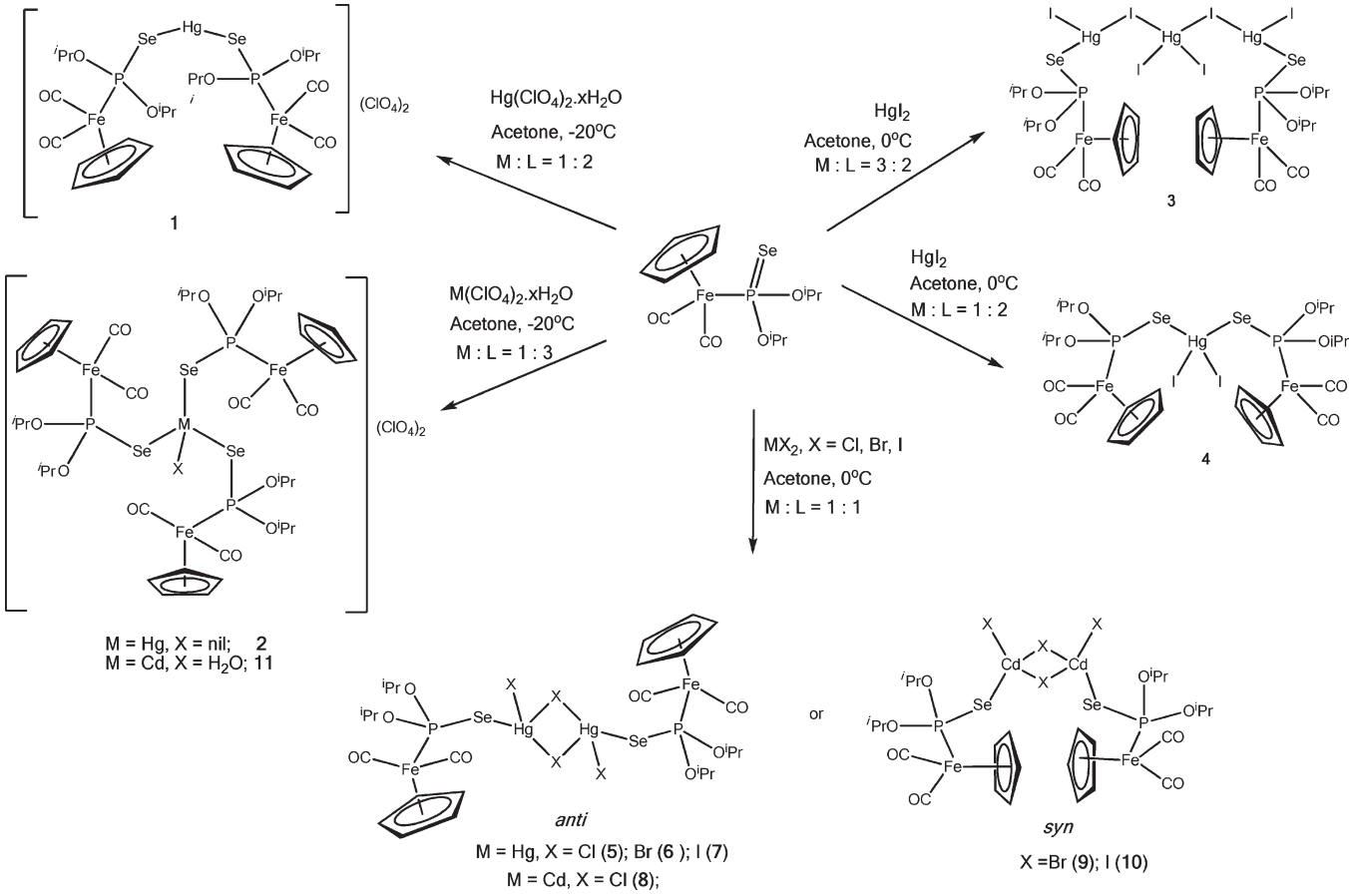

of a metallo supramolecular species (Figure 2b). The distance between the centroids of the Cp rings, 3.416(16) Å, lies well within the reported range for that of the π-stacked rings (3.3−3.8 Å).[22] It is noted that all three bulky Cp rings remain at one side of the Se_3 plane, and π-stacking of Cp rings may account for this type of arrangement in the solid state.

Compound 4. The asymmetric unit contains two independent molecules of a neutral cluster $[HgI_2L_2]$. Figure 3 depicts only one of them, in which the four-coordinated Hg(II) is bonded to two Se atoms of **L** and two I atoms. The geometry of Hg centers in both molecules is distorted tetrahedral. Hg−Se lengths in **4** are the largest among this series but remain within the lengths [2.717(2)−2.796(2) Å] observed in $[\{PhSe_2(CH_2)_2O(CH_2)_2O\}_2Hg_2I_4]$.[23] In contrast, the Hg−I distances [2.7044(10)−2.7785(11) Å] are shorter than those reported in **3** [2.762(1)−3.087(1) Å]. The P−Se−Hg angles [104.90(9)− 119.40(9)°] are larger than those in compound **3**.[4] A similar HgI_2Se_2 coordination environment is also identified in $[\{(Ph_2PSe)_2CH_2\}HgI_2]$,[8b] $[(C_4H_8Se)_2HgI_2]$,[24] and $[\{PhSe_2(CH_2)_2O(CH_2)_2O\}_2Hg_2I_4]$.[23]

Compound 5. The perspective view of the molecule is shown in Figure 4a. Two Hg and two Cl atoms form a parallelogram core with edge lengths of 2.610(3) and 2.742(4) Å and angles of 93.84(9)° and 86.16(9)°. Each Hg is coordinated by one Se, two bridging Cl's, and a terminal Cl atom in a distorted tetrahedral fashion. The $Hg-Cl_{terminal}$ distance, 2.392(4) Å, is comparably shorter. The **L** ligand unit is coordinated to Hg via its Se atom, and two $[LHgCl_2]$ units dimerize to form **5**, having an inversion center. The Hg−Se distance of 2.4931(19) Å is shorter and the P−Se distance of 2.229(3) Å is longer than those observed in **2**, **4**, and **6**. In the literature, only three compounds, $[HgCl(\mu\text{-}Cl)(C_4H_8Se)]_2$,[25a] $[HgCl(\mu\text{-}Cl)(MeSeCH_2SiMe_3)]_2$,[25b] and $[HgCl(\mu\text{-}Cl)(SePPh_3)]_2$,[26] have a Hg_2Cl_2 parallelogram core and display a binding mode of $HgSeCl_3$. Structural comparison reveals that the Hg−Se length, 2.53(3) Å, is 0.036 Å longer and the P−Se distance, 2.17(4) Å, is 0.056 Å shorter in $[HgCl(\mu\text{-}Cl)(SePPh_3)]_2$ than those observed in **5**. Hence, the lower (+3) oxidation state of P in **5** caused a longer P−Se length. Therefore, the greater electron density remaining on the Se atom effectively forms a stronger bond with the metal and results in a shorter M−Se distance in **5**. In addition, the Hg−Se distance in $[HgI(\mu\text{-}I)(SePPh_3)]_2$

(22) (a) Janiak, C. *J. Chem. Soc., Dalton Trans.* **2000**, 3885–3896. (b) Stoffregen, S. A.; Vecchi, P. A.; Ellern, A.; Angelici, R. J. *Inorg. Chim. Acta* **2007**, *360*, 1711–1716.
(23) Mazouz, A.; Meunier, P.; Kubicki, M. M.; Hanquet, B.; Amardeil, R.; Bornet, C.; Zahidi, A. *J. Chem. Soc., Dalton Trans.* **1997**, 1043–1048.
(24) Stalhandske, C.; Zintl, F. *Acta Crystallogr., Sect. C* **1988**, *44*, 253–255.
(25) (a) Stalhandske, C.; Zintl, F. *Acta Crystallogr., Sect. C* **1986**, *42*, 1449–1450. (b) Chadha, R. K.; Drake, J. E.; McManus, N. T.; Mislankar, A. *Can. J. Chem.* **1987**, *65*, 2305–2311.
(26) McQuillan, G. P.; Glasser, L.; Ingram, L.; King, M. G. *J. Chem. Soc. A* **1969**, 2501–2504.

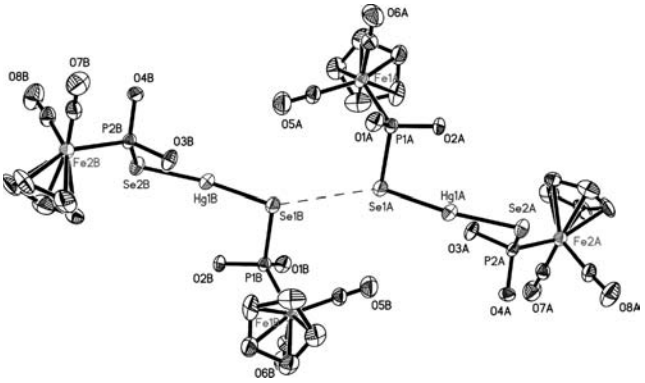

Figure 1. The Se···Se secondary interaction identified in **1** (with isopropyl groups omitted for clarity).

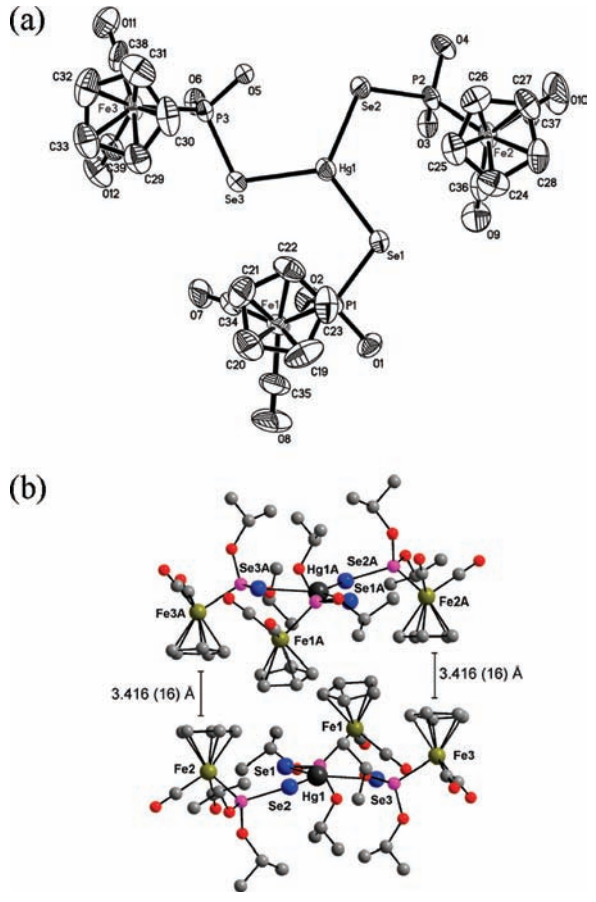

Figure 2. (a) A perspective view of the dicationic cluster in **2** with isopropyl groups omitted for clarity. (b) The π-stacking of two of the Cp rings of neighboring molecules, identified in **2**.

(2.5914(11) Å)[8d] is 0.098 Å longer than those in **5**, while the P−Se distance (2.173(3) Å) is 0.056 Å shorter. The bond angles around the P, ranging from 106.16(33) to 112.10(22)° in $[HgCl(\mu\text{-}Cl)(SePPh_3)]_2$ and 106.1(4) to 112.7(3)° in $[HgI(\mu\text{-}I)(SePPh_3)]_2$, are comparable. On the other hand, bond angles around the P atom in **5** are distributed in a wider range, 100.7(3)° [O2−P1−O1] to 122.11(12)° [Fe1−P1−Se1]. However, this difference may not be attributable strictly to the nature of P because the size of the substituent atoms also has some effect. Thus, the P−Se−Hg angles, 97.97(27)° in $[HgCl(\mu\text{-}Cl)(SePPh_3)]_2$, 98.04(7)° in $[HgI(\mu\text{-}I)(SePPh_3)]_2$, and 97.55(8)° in **5**, are very much similar.

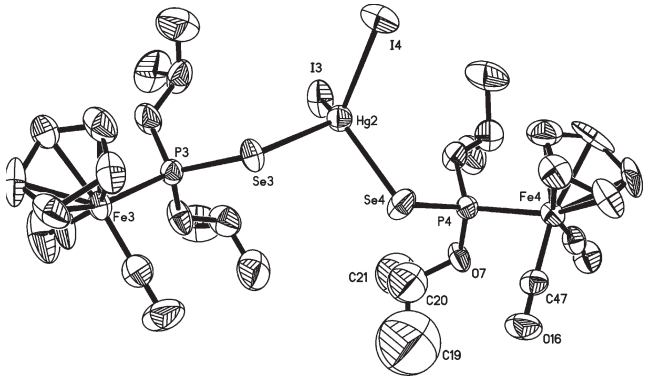

Figure 3. A perspective view of the compound in **4**.

Both intra- and intermolecular H-bonding between Cl atoms and Cp hydrogen atoms are revealed in the packing motif of **5** (Figure 4b). The H-bonding parameters are listed in Table 5. The distances observed in **5** are within the reported C−H···Cl−ML_n hydrogen-bonding distances (2.987 Å), as calculated by van den Berg and Seddon.[27] The copper complex containing the **L**, $[Cu(\mu\text{-}Cl)(L)]_2$, also exhibited intermolecular H-bonding between Cp protons and bridging Cl atoms of neighboring molecules to form a 1D chain.[6] The torsion angle (Hg1−Cl1−C14−C15) of 83.13(17)°, a measurement of relative orientation of the Cp ring and Hg_2Cl_2 parallelogram core, indicates that these planes are nearly perpendicular to each other. It should be noted that the dihedral angle between the Cp ring and the central parallelogram core observed in $[Cu(\mu\text{-}Cl)(L)]_2$ was 24.62° but was 84.58° in $[Cu(\mu\text{-}Br)(L)]_2$.[6]

Compound 6. The structure of **6** is isomorphous with **5**. The $Hg-Br_{bridging}$ (2.7184(6), 2.8745(6) Å) as well the $Hg-Br_{terminal}$ bond lengths (2.5042(7) Å) are comparable to those observed in $[HgBr(\mu\text{-}Br)(MeSeCH_2SiMe_3)]_2$,[25b] the only predecessor containing a Hg_2Br_2 core in which each Hg is further coordinated to a Se atom.

With the exception of **4**, all other Hg complexes exhibit comparable P−Se−Hg angles as that observed in **3**.[4] P−Se distances [2.158(5), 2.146(6) Å] and Hg−Se lengths [2.693(8), 2.651(9) Å] in $[\{(Ph_2PSe)_2CH_2\}HgBr_2]$ are ~0.07 Å shorter and ~0.14 Å longer than those in **6**, respectively [P−Se, 2.2276(13); Hg−Se, 2.5151(6) Å], which is reminiscent of the difference between secondary and tertiary phosphine selenide complexes mentioned above.

An alternative explanation for the longer P−Se bond could be that the balance between electron-releasing actions of the electropositive organo-iron and electronegative isopropoxyl substituents might have induced better donor properties in the phosphine selenide **L**, which would have formed stronger as well as shorter Hg−Se bonds with subsequent P−Se bond elongation. Comparison of the reference compound $[Hg\{Se_2P(O^iPr)_2\}_2]_n$,[9a] with **4** reveals that such an assumption may not be true. Three out of four Hg−Se lengths in $[Hg\{Se_2P(O^iPr)_2\}_2]_n$ [2.544(2), 2.663(2), and 2.611(2) Å] are either shorter or comparable to those in **4** [2.7667(14), 2.7700(14), 2.6448(15), and 2.6394(15) Å]. Still, all of the P−Se distances in **4** [2.162(4)−2.176(3) Å] are longer than those

(27) van den Berg, J.-A.; Seddon, K. R. *Cryst. Growth Des.* **2003**, *3*, 643–661.

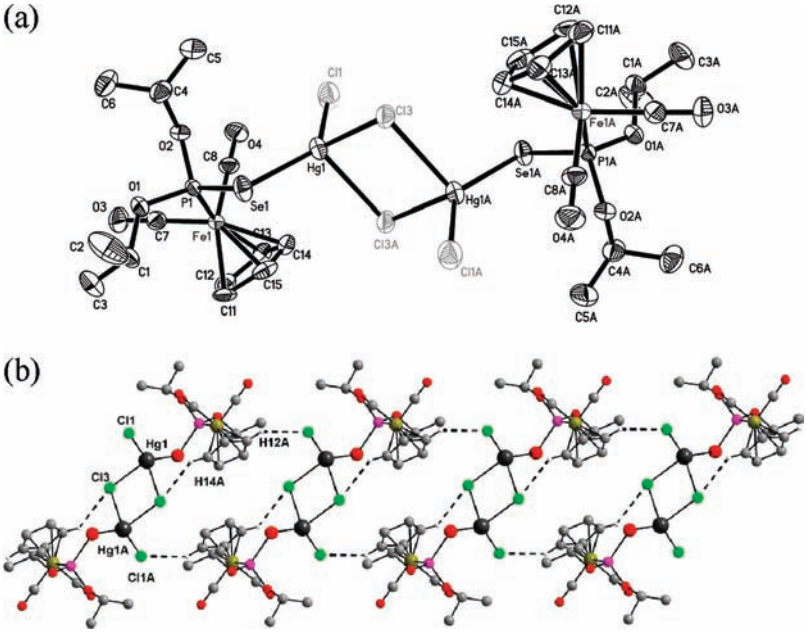

Figure 4. (a) A perspective view of $[HgCl(\mu\text{-}Cl)\{CpFe(CO)_2P(Se)(O^iPr)_2\}]_2$, **5**. (b) Both intra- and intermolecular C−H···Cl H-bonding in the packing motif of **5**.

Table 5. Hydrogen-Bonding Parameters for **5** and 8−**10**[a]

D−H···A	H···A/Å	D···A/Å	D−H···A/deg	symmetry operation for A
		Complex **5**		
C14−H14A···Cl3A	2.87(3)	3.551(43)	127	$1-x, -y, 1-z$
C12−H12A···Cl1	2.88(3)	3.531(31)	125	$x, 1+y, z$
		Complex **8**		
C3−H3···Cl1	2.85(1)	3.808(19)	167	$x, -1+y, z$
C5−H5···Cl1	2.83(2)	3.738(21)	155	$x, 0.5-y, 0.5+z$
		Complex **9**		
C5−H5···Br1	2.99(0)	3.962(8)	172	$-x, -0.5+y, 0.5-z$
C18−H18···Se2	2.82(0)	3.768(9)	163	$1-x, 0.5+y, 0.5-z$
		Complex **10**		
C4−H4A···I1	3.09(0)	4.052(8)	167	$1.5-x, 0.5+y, z$
C1−H1A···Se1	3.07(0)	3.832(8)	135	$1+x, y, z$

[a] D−H lengths are 0.98 Å for all of the cases.

[2.142(4)−2.160(4)Å] in the reference compound. In fact, all P—Se lengths observed in **1**−**6** [2.161(3)−2.231(4) Å] are longer than those observed in $[Hg\{Se_2P(O^iPr)_2\}_2]_n$,[9a] containing P^V.

P−Se distances [2.161(3)−2.176(3) Å] in **4** are shorter than those observed in **5** (2.229(3) Å) and **6** (2.2276(13) Å), which suggest that the $^{31}P-^{77}Se$ coupling constant observed in **4** should be larger than those in **5** and **6** (vide infra).

Compound 8. The Cd complex is isostructural with the Hg complex **5**. The molecule also contains an inversion center. Each Cd is coordinated to a "Se", a terminal "Cl", and two bridging "Cl" atoms in a distorted tetrahedral geometry. $Cd-Cl_{bridging}$ [2.494(2) and 2.623(2) Å] and $Cd-Cl_{terminal}$ (2.410(2) Å) distances lie in the range reported for the compound $[CdCl(\mu\text{-}Cl)L]_2$, where L = 2,6-bis(methylthiomethyl)pyridine.[28] The Cd−Se distance, 2.5771(16) Å, in **8** is the shortest in the series of **8**−**11**.[4] The P−Se length, 2.187(2) Å, is shorter than those observed in its mercury analogs, **5** and **6**. The 2-D network, which was revealed in the crystal lattice of **8** and formed by hydrogen bonding, is presented in Figure 5, and the parameters are listed in Table 5. It is noted that the calculated cutoff value for $C-H\cdots Cl-MZ_n$ is 2.987 Å.[27]

Compound 9. A perspective view of the molecule is shown in Figure 6a. Both Cd centers are surrounded by a "Se", a terminal "Br", and two bridging "Br" atoms in distorted tetrahedral fashion. Unlike **8**, which reveals a planar Cd_2Cl_2 core, two Cd atoms and two bridging Br atoms form a puckered Cd_2Br_2 tetragon. The torsion angle, the amount of distortion from planarity for this tetragon, is 157.22(4)° for Cd2−Br2−Br3−Cd1. The

(28) Lai, W.; Berry, S. M.; Bebout, D. C.; Butcher, R. J. *Inorg. Chem.* **2006**, *45*, 571–581.

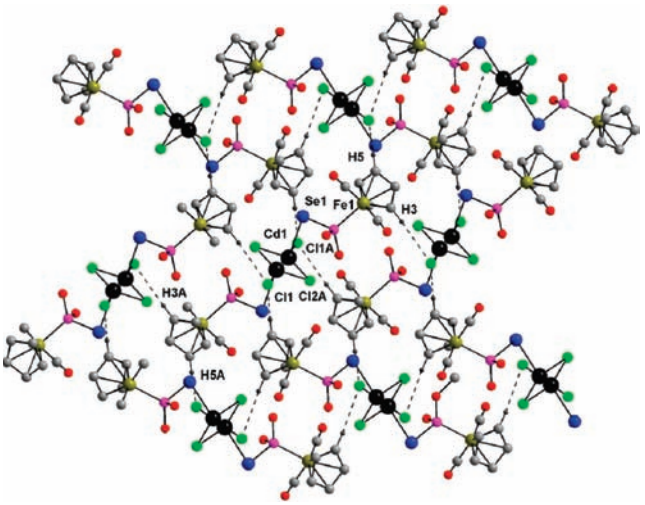

Figure 5. 2D network formed by H-bonding interactions in the lattice of compound **8**. Isopropyl groups are omitted for clarity.

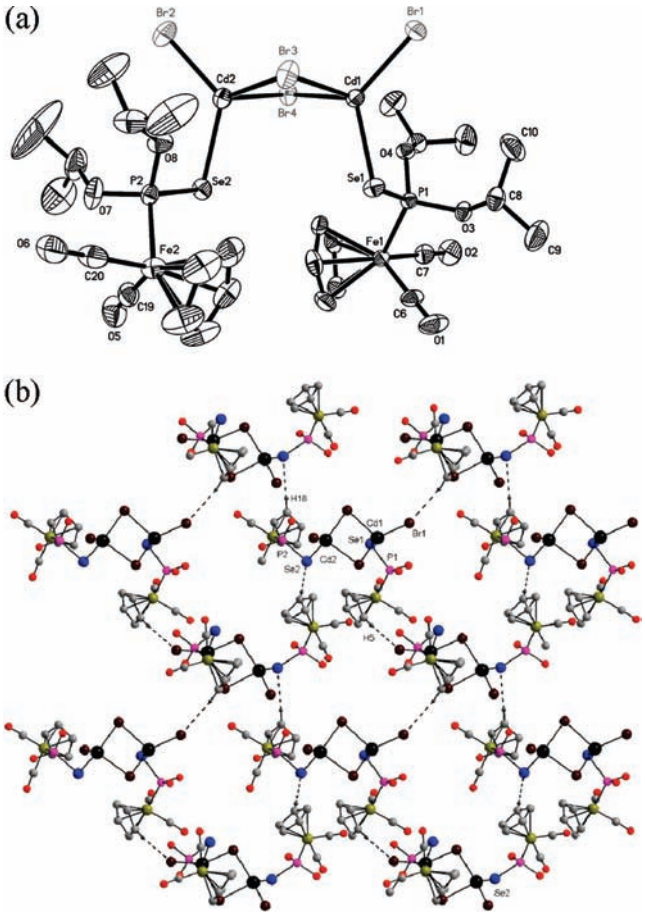

Figure 6. (a) A perspective view of $[CdBr(\mu\text{-}Br)\{Cp(CO)_2FeP(Se)(O^iPr)_2\}]_2$, **9**. (b) 2D-network formed by H-bonding interactions in the lattice of compound **9**. Isopropyl groups are omitted for clarity.

$Cd-Br_{bridging}$ distances [2.6214(9)−2.7488(9) Å] in the tetragon are comparable with those observed in $[Cd_2Br_4(PSiMe_3)_2]$[29] with a planar Cd_2Br_4 core. Shorter $Cd-Br_{terminal}$ distances, 2.5110(9) and 2.5207(8) Å, are also reminiscent of those observed in $[Cd_2Br_4(PSiMe_3)_2]$.[29] Two Cd−Se lengths, 2.5925(7) and 2.6033(8) Å, are also comparable to those reported in **11**.[4] More importantly, the two bulky "**L**" ligand units, which coordinate via their Se atoms to the Cd of the Cd_2Br_2 tetragon, are in pseudo-syn orientation (Figure 6a). Although the formation of a M_2X_2 tetragon (X = halide) and the further participation of these metal centers in coordination to other ligands is a common phenomenon in coordination chemistry, the spatial disposition of those ligands being syn is rare.

A strong nonbonding interaction is revealed between Cd and isopropoxyl oxygen with distances of 2.870(5) and 2.901(5) Å for Cd(1)···O(4) and Cd(2)···O8, respectively. Eventually, a 2-D network is revealed in the lattice of **9**, via H-bonding interactions, which is presented in Figure 6b. The H-bonding distances observed in **9** are shorter than both the calculated limiting values for $C-H\cdots Br-MZ_n$ (3.123 Å)[27] and the reported $C-H\cdots Se$ distances.[30] These secondary interactions might account for the puckered Cd_2Br_2 core and the subsequent syn orientation of the bulky ligands as well.

Compound 10. Compound **10** is isostructural with compound **9**. The two bridging I atoms and the two Cd atoms form a nonplanar Cd_2I_2 tetragon, and ligand **L** is attached through its Se to each of the Cd atoms. The torsion angle of Cd1−I1A−I1−Cd1A is 149.30(3)°. Thus, each Cd is coordinated by two bridging I, a terminal I, and a Se atom. $Cd-I_{bridging}$ [2.8452(6) and 2.9124(7) Å] as well as $Cd-I_{terminal}$ lengths [2.6960(7) Å] are shorter than those observed in $[CdI_2(Pyzca)(H_2O)]_\infty$ [2.8275(7)−3.0122(7) Å, Pyzca = 2-pyrazinecarboxylic acid].[31] The Cd−Se distance, 2.6066(8) Å, lies in the reported range for the compound $[Cd\{Se_2P(O^iPr)_2\}_2]_2$.[9a] The P−Se bond distance, 2.1857(16) Å, is comparable with that in the previously reported Cd complex, **11**.[4]

Slipped $\pi-\pi$ interactions between the Cp rings of the neighboring molecules are confirmed by the distance of 3.332(0) Å between the centroid of the rings (Figure 7).[22] H-bonding distances (Table 5) in the lattice lie below the calculated $C-H\cdots I-MZ_n$ (3.351 Å)[27] and reported $C-H\cdots Se$[30] distances.

A tertiary, phosphine selenide cadimum complex, isostructural to **8**−**10**, has not been reported to date. So, we made a structural comparison of the Cd compounds with $[\{(Ph_2PSe)_2N\}_2Cd]$,[8e] which reveals that P−Se bonds in the reference compound [2.163(2)−2.173(2) Å] are slightly shorter than those in **8**−**10** (2.1738(16)−2.187(2) Å) and Cd−Se distances [2.6170(8)−2.6415(8) Å] are longer than those observed in **8**−**10** [2.5771(16)−2.6066(8) Å], which is reminiscent of the result observed in the Hg(II) complexes. The P−Se lengths [2.125(6)−2.144(5) Å; 2.134(6) Å (av.)] in $[Cd_2\{Se_2P(O^iPr)_2\}_4]$,[9a] containing P^V, are also ∼0.05 Å shorter than those identified in **8**−**10**.

(29) Fuhr, O.; Fenske, D. *Z. Anorg. Allg. Chem.* **1999**, *625*, 1229–1236.

(30) (a) Iwaoka, M.; Tomoda, S. *J. Am. Chem. Soc.* **1994**, *116*, 4463–4464. (b) Salon, J.; Sheng, J.; Jiang, J.; Chen, G.; Caton-Williams, J.; Huang, Z. *J. Am. Chem. Soc.* **2007**, *129*, 4862–4863. (c) Narayanan, S. J.; Sridevi, B.; Chandrashekar, T. K.; Vij, A.; Roy, R. *Angew. Chem., Int. Ed.* **1998**, *37*, 3394–3397.

(31) Ciurtin, D. M.; Smith, M. D.; zur Loye, H.-C. *Polyhedron* **2003**, *22*, 3043–3049.

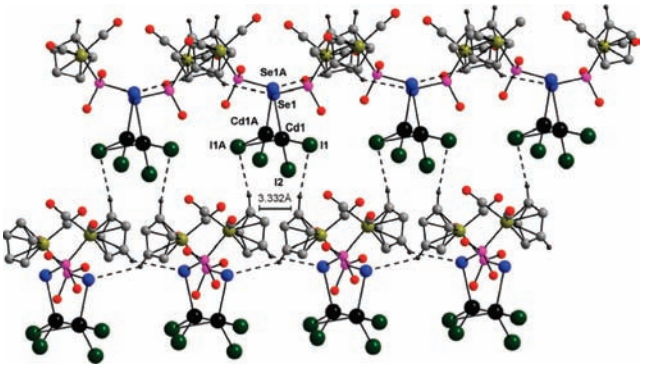

Figure 7. 2D-network formed in the lattice of **10** by H-bonding and $\pi-\pi$ interactions. Isopropyl groups are omitted for clarity

Whereas all of the halide anions engage themselves in the primary coordination sphere of the Hg(II) and Cd(II) complexes, mercury complexes of **1** and **2**, as well as the Cd compound in **11**, have the perchlorate counteranion outside the coordination sphere.

NMR Studies. Each of the compounds **1**−**7** exhibits a set of doublet and multiplet resonances from the methyl and methine protons of the isopropyl group, respectively, in addition to a singlet from the Cp rings in the ^{1}H NMR spectrum, which suggests that all of the ligand units present in a particular complex are chemically equivalent on the NMR time scale. This is supported by the room-temperature ^{31}P NMR spectra of **1**−**7**, which show only a singlet flanked by a pair of satellites originating from the ^{31}P−^{77}Se coupling. A decrease in the coupling constant ($^1J_{PSe}$), with respect to the uncomplexed metalloligand (**L**) (J_{PSe} = 712.9),[4] is observed in all of the compounds **1**−**7**, which can indicate that the P−Se bond order should be decreased along with the formation of the mercury−selenium bond. This is further evidenced from the smaller value of J_{PSe} for **1**, as compared to that for **2**, which can be correlated by the fact that a Hg(II) center is coordinated to only two ligands in **1**, as compared to three ligands in **2**. The difference in bond order is also reflected in the P−Se bond lengths (vide supra). Interestingly, the addition of 1 equiv of ligand **L** to compound **1** in solution leads to the formation of compound **2**, which is confirmed by ^{31}P NMR. Furthermore, compounds **1** and **2** show a singlet flanked by two pairs of satellites in the ^{31}P NMR spectrum at −60 °C. The origin of the additional set of satellites arises from the two-bond coupling of ^{199}Hg−^{31}P nuclei. This fact further indicates the magnetic equivalency of the selenophosphito ligand moieties in **1** and **2** in solution, even at a temperature as low as −60 °C.

All of the Hg complexes (**1**−**7**) exhibit only one doublet, shifted downfield, as compared to the precursor **L** (δ = 199.6 ppm),[4] in the ^{77}Se NMR spectra. It is interesting to note that, since each Hg(II) is coordinated by one Se and three halides in **5**−**7**, the different electronic effects between halides do not cause great changes in the P−Se coupling constant (J_{SeP} values for **5**, **6**, and **7** are 532.7, 546.1, and 570.6 Hz, respectively). On the other hand, the Hg(II) is surrounded by two Se and two iodides, shown in **4**, exhibiting the largest J_{PSe} (643.9 Hz), as compared to those observed in both **5** and **6**, which suggests a larger P−Se bond order in **4** (vide supra). The P−Se coupling constants measured from the ^{77}Se spectrum are in good agreement with those obtained from the ^{31}P NMR spectrum. It is surprising that no chemical shift in ^{77}Se NMR spectra could be observed for both **5** and **6** in solvents other than DMSO.

Although efforts have been made to synthesize both chloro- and bromo- analogs of **3** and **4** by varying the metal-to-ligand ratio, the solution-state ^{31}P NMR experiments did not explicitly indicate the formation of other heterometallic complexes, with the exception of **5** and **6**. On the other hand, McQuillan et al. reported a chloro-bridged, dimeric structure of [HgCl(μ-Cl)(SePPh$_3$)]$_2$,[26] having a $Hg_2Cl_4Se_2$ skeleton, which was similar to that observed in **5**. Lobana et al. used the same tertiary phosphine−selenide ligand to obtain [Hg(μ-I)I(Ph$_3$PSe)]$_2$ containing a $Hg_2I_4Se_2$ moiety.[8d] Thus, we anticipate that [HgI$_2$L]$_2$, **7**, formed by the complexation of **L** with HgI$_2$ in a 1:1 ratio, would be isostructural with its chloro (or bromo) analog of **5** (or **6**). Surprisingly, repeated recrystallization of **7** always gives rise to single crystals of **3**, and some residues with compositions of a mixture of **4** and **7**. Presumably, the dimeric species of **7** is in equilibrium with **3** and **4** in solution (eq 1). However, the solubility of **3** is comparably less in common organic solvents, while both **4** and **7** are highly soluble. Hence, **3** crystallizes out first, which shifts the equilibrium toward the right and leaves the mixture of compounds of **4** and **7** in solution.

$$2[HgI_2L]_2\ (\mathbf{7}) \leftrightarrows [Hg_3I_6L_2]\ (\mathbf{3})\downarrow + [HgI_2L_2]\ (\mathbf{4})\ldots \quad (1)$$

The 1:1 mixture of **3** and **4** in acetone exhibits a single peak, with a pair of selenium satellites at ∼175 ppm, close to that of **7** in the ^{31}P NMR spectrum, and the observed J_{PSe} (∼580 Hz) does not correspond to any of the compounds in **3** or **4** but is closer to **7** (570.6 Hz). These facts further rationalize our postulation regarding the solution-state equilibrium of these three compounds.

In a similar manner to that observed for the mercury compounds, each of the Cd compounds in **8**−**10** exhibits a single set of chemical shifts, either for the methyl or for the methine protons. The ^{31}P NMR spectrum of each of the compounds in **8**−**10** exhibits a singlet peak with a pair of selenium satellites at room temperature. Although doublet peaks are observed in the ^{77}Se NMR spectrum for **9** and **10**, surprisingly, two overlapping doublet peaks, centered at 167.5 and 172.4 ppm, are identified for **8**, suggesting slightly different chemical environments for the two Se nuclei. The coupling constants obtained from ^{77}Se and ^{31}P NMR are comparable for **9** and **10** but not for the compound in **8**. In addition to this, an approximately 100 Hz larger J_{PSe} value for **8**, compared to those in **9** and **10** in ^{31}P NMR spectra, prompts us to explore the potential lability of Cd−Se bonds in solution, via a variable-temperature (VT) NMR technique. VT ^{31}P NMR spectra of **9** and **10** shows peak broadening and downfield shifting to ∼180 ppm, with a nearly unaltered J_{PSe} upon gradual cooling to −90 °C. A similar observation was made for **8** (Figure S1, Supporting Information) in acetone-d$_6$ upon cooling up to −50 °C. Upon further cooling to −90 °C, **8** exhibits two peaks, at 176.8 ppm (J_{PSe} = 602.2 Hz) and 170.7 ppm (J_{PSe} = 720.0 Hz), and each is associated with a pair of Se

satellites in an approximately 1:3 integration ratio. The J_{PSe} for the peak at 176.8 ppm is comparable to those of **9** and **10**, but the J_{PSe} at 170.7 ppm is comparable to that of the uncoordinated metalloligand "**L**".[4] It is unlikely that **8** can maintain its intact solid-state structure in solution at room temperature; instead, it remains in a dynamic equilibrium with free ligand (**L**) in a 1:3 ratio. In a similar experiment in CD_2Cl_2 (Figure S2, Supporting Information), **8** shows a singlet at 170.9 ppm (J_{PSe} = 635.4 Hz) with selenium satellites at room temperature, which splits into two singlets of 174.9 (J_{PSe} = 593.7 Hz) and 170.2 ppm (J_{PSe} = 709.2 Hz) at −90 °C, with approximately a 3:1 integration ratio, suggesting that the amount of intact molecules in **8** increases in lower-polarity solvent CD_2Cl_2. Since there is no significant difference in either Cd−Se or P−Se lengths in **8**−**10** (vide infra), the coupling constant difference can be attributed to the intrinsic lability of the Cd−Se bond in compound **8**.

It is interesting to note that the $^{31}P-^{77}Se$ coupling constants of the Hg complexes in **5** and **6** are smaller (∼532 and 548 Hz), as compared to those of analogous Cd complexes in **8**−**10**; that is, the P−Se lengths are greater than those in the Cd complexes of **8**−**10**. This is justified according to the P−Se lengths of 2.229(3) Å in **5** and 2.2276(13) Å in **6**, which are longer than 2.174 (2)−2.187(2) Å in **8**−**10**.

Infrared Spectroscopy. All of the complexes (**1**−**11**) exhibit two bands, a characteristic for metal-bound carbonyl stretching, in infrared spectroscopy (vide infra). In addition, the P−Se stretching frequency was also identified for these compounds in the range 517−530 cm^{-1} (see Experimental Section). The lowest peak at 517 cm^{-1} was observed for $[HgCl(\mu\text{-}Cl)L]_2$, **5**. The mercury compounds (**1**−**7**) exhibit a P−Se stretching frequency in the range 517−528 cm^{-1}, which is slightly lower than those of cadmium compounds **8**−**11** (528−530 cm^{-1}). Although the stretching frequency of P−Se in free **L** (538 cm^{-1}) is shifted to a lower value in the complexes, as expected, the magnitude of the shifts is not enough to make a correlation with the individual P−Se bond lengths of the complexes obtained from crystallography. However, the P−Se stretching frequency (562 cm^{-1})[32] in PPh_3Se, the ligand used in the reference compound $[HgCl(\mu\text{-}Cl)(SePPh_3)]_2$, which is ∼24 cm^{-1} larger than that of free **L**, does display a bond strength difference between the secondary and tertiary ligands.

Electrochemistry Studies. The large separation observed between the anodic (0.90 V) and cathodic (−0.30 V) peaks in the cyclic voltammogram of **1** in acetonitrile (Figure S3, Supporting Information) suggests that these peaks are not associated with a reversible oxidation−reduction process. The peak positions also get shifted upon variation of the scan rate. This indicates that oxidation is followed by a rapid chemical process. Presumably, the oxidation at 0.90 V leads to the formation of a species containing dicarbonyl−iron(III), which might lose a CO ligand to generate a monocarbonyl−Fe (III) species. This transient compound eventually gets reduced at −0.30 V, to show the irreversible reduction peak. The cyclic voltammogram of the free ligand **L** also shows the same pattern, but oxidation and reduction take place at less positive and less negative potentials, suggesting the ease of the redox process in the free ligand, as expected. Cuadrado et al. reported similar electrochemical behavior for $Cp(CO)_2FeSi(Me)_2CHCH_2$ in a cyclic voltammetry experiment.[33] Other compounds also exhibit a qualitatively similar pattern in their cyclic voltammograms. However, the complexes containing halides (**3**−**10**) show additional irreversible oxidation peaks, presumably originating from oxidation of the dissociated halide ions. It is noted that bromide- and chloride-containing species showed one additional peak, but iodide-containing complexes (**3**, **4**, **7**, and **10**) showed two additional peaks, reminiscent of the two-step oxidation of iodide to triiodide and then iodine typically observed in nonaqueous solvents.[34] The electrochemical parameters are listed in Table 6. We have found some solid residue after the experiments, which suggests decomposition of the compounds during the redox process. Thus, we cannot speculate much to correlate the bond lengths data with the redox behavior of the individual complexes.

Table 6. Redox Potential (V vs $FeCp_2^{0/+}$) of **L** and complexes **1**−**11**

compd	E_A	E_C	compd	E_A	E_C
L	0.81	−0.05	**6**	0.90, 0.36	−0.28
1	0.90	−0.30	**7**	0.82, 0.30, 0.01	−0.26
2	0.89	−0.43	**8**	0.95, 0.34	−0.65
3	0.84, 0.34, 0.03	−0.46	**9**	0.92, 0.32	−0.63
4	0.83, 0.34, 0.08	−0.50	**10**	0.84, 0.38, 0.04	−0.59
5	0.85, 0.38	−0.30	**11**	1.02	−0.56

Concluding Remarks

This paper demonstrates that the mercury complexes of $[CpFe(CO)_2P(Se)(O^iPr)_2]$, **1**−**7**, synthesized from perchlorate and halide salts of Hg(II), can exhibit different coordination geometries and binding modes. The less-coordinating nature of $[ClO_4]^-$ results in the formation of dicationic complexes of both $[ML_2]^{2+}$ and $[ML_3]^{2+}$ (**1** and **2**), which contain either two- or three-coordinate Hg(II), depending on the metal-to-ligand ratio used. Bulky Cp rings in **1** and **2** reside in an apparent syn orientation due to several nonbonding secondary interactions. In contrast, halide salts produce neutral complexes with a higher coordination number of mercury, as the more coordinating nature of halides engages them in the coordination sphere in addition to the selenium donor ligand. The higher metal-to-ligand ratio yields a $M_3I_6L_2$ type of complex, **3**, with a higher metal content,[4] whereas the lower metal-to-ligand ratio results in the formation of a MI_2L_2-type complex, **4**. Equimolar HgX_2 (X = Cl, Br, I) produces $[MX_2L]_2$ types of compounds, **5**−**7**. Thus, only the iodide as an ancillary ligand allowed flexibility in the coordination sphere of Hg in terms of the number of metal atoms, similarly to the coordination environment's effect on variations of stoichiometry; however, the use of Cl^- and Br^- as the auxiliary ligands only allowed the formation of a complex with a 1:1 metal-to-ligand ratio irrespective of the stoichiometric ratio of the starting materials used. The

(32) Carr, S. W.; Colton, R. *Aust. J. Chem.* **1981**, *34*, 35–44.

(33) Ramírez-Oliva, E; Cuadrado, I; Casado, C. M.; Losada, J.; Alonso, B. *J. Organomet. Chem.* **2006**, *691*, 1131–1137.

(34) Munisamy, T.; Gipson, S. L. *J. Organomet. Chem.* **2007**, *692*, 1087–1091.

solution state equilibrium of **3**, **4**, and **7** is demonstrated, which might be responsible for the growth failure of single crystals of **7**. It is worth noting that $\{CpFe(Cp(Se)(CH(CH_3)N(CH_3)_2)\}_2Hg$,[35] is the only known iron−mercury heterometallic compound with a Se connected to the mercury atom, aside from that in **1**−**7**.

In a similar manner to that for the mercury complexes, the perchlorate salt of Cd(II) produced a dicationic $[CdL_3(H_2O)]^{2+}$ complex of **11**.[4] However, the CdX_2 (X = halide) generated neutral complexes in **8**−**10**, where halides are being incorporated in a metal coordination sphere. However, attempts to identify species other than **10** by varying the metal-to-ligand ratio failed, in contrast to the variety of products isolated in the case of HgI_2. The chloro compound in **8** is isostructural with its mercury analogue of **5**. Even though the bromo and iodo homologs in **9** and **10** have similar bonding patterns as **8**, they differ in the spatial arrangement of the bulky "**L**" units and the lack of planarity of the central Cd_2X_2 unit. The unusual syn conformation of the bulky ligand units may be attributable to weak nonbonding interactions. In addition, the solution VT ^{31}P NMR clearly suggests that the Cd−Se bond in **8** is labile.

That the P atom in the secondary phosphine selenides has +3 oxidation number is known without a doubt.[5a] A profound structural characteristic uncovered in this study is that the P−Se bond lengths are longer in secondary phosphine selenide metal complexes than those containing tertiary phosphine selenide or phosphorus diselenide, which can be lineated with the lower formal oxidation state of the P atom in these complexes. We also found shorter Hg(Cd)−Se bonds in these complexes resulted from the better donor property of the ligand **L** compared to referenced phosphine selenide Ph_3PSe.

Acknowledgment. We thank the National Science Council of Taiwan (NSC 97-2113-M-259-007-MY3) for financial support.

Supporting Information Available: X-ray crystallographic files in CIF format for compounds **1**, **2**, **4**−**6**, **8**−**10**; VT ^{31}P NMR of **8** in acetone-d_6 (S1) and CD_2Cl_2 (S2); and the cyclic voltammogram of **1** (S3) are available free of charge via the Internet at http://pubs.acs.org.

(35) Kaur, R.; Singh, H. B.; Patel, R. P.; Kulshreshtha, S. K. *J. Chem. Soc., Dalton Trans.* **1996**, 461–466.